Short communication

Molecular cloning and characterization of marmoset aldehyde oxidase

Shotaro Uehara, Yasuhiro Uno, Eriko Okamoto, Takashi Inoue, Erika Sasaki, and Hiroshi Yamazaki

Laboratory of Drug Metabolism and Pharmacokinetics, Showa Pharmaceutical University, Machida, Tokyo 194-8543, Japan (SU, EO, and HY); Pharmacokinetics and Bioanalysis Center, Shin Nippon Biomedical Laboratories, Ltd., Kainan, Wakayama, Japan (YU); Department of Applied Developmental Biology (TI) and Center of Applied Developmental Biology (ES), Central Institute for Experimental Animals, Kawasaki, Japan; and Keio Advanced Research Center, Keio University, Minato-ku, Tokyo, Japan (ES)

DMD Fast Forward. Published on May 9, 2017 as DOI: 10.1124/dmd.117.076042
This article has not been copyedited and formatted. The final version may differ from this version.

Running Title Page

Running title: Cloning of marmoset AOX1 cDNA

Correspondence author: Hiroshi Yamazaki, PhD, Professor

Showa Pharmaceutical University, 3-3165 Higashi-tamagawa Gakuen, Machida, Tokyo 194-8543, Japan. Phone: +81-42-721-1406; Fax: +81-42-721-1406. E-mail: hyamazak@ac.shoyaku.ac.jp

Number of Text Pages : 17

Number of Tables : 1

Number of Figures : 1

Number of References : 14

Number of Words in Abstract : 235

Number of Words in Introduction : 294

Number of Words in Rusults & Discussion : 993

Abbreviations: AOX, aldehyde oxidase (EC 1.2.3.1); HPLC, high performance liquid chromatography; PCR, polymerase chain reaction; RT, reverse transcription.

Abstract

Common marmosets (*Callithrix jacchus*), New world monkeys, are a promising primate model for preclinical drug metabolism studies due to the similarities of cytochrome P450 (P450) enzyme function to those of humans. Despite an increasing number of drug candidates catalyzed by non-P450 enzymes, drug metabolizing enzymes other than P450s have been hardly identified or characterized in marmosets. In this study, we identified *aldehyde oxidase* (*AOX*) *1* gene by marmoset genome analysis. AOX1 cDNA was cloned from marmoset livers by reverse transcription-polymerase chain reaction. Deduced amino acid sequences of AOX1 cDNA showed high sequence identities (92–93%) with primate AOX1s. Phylogenetic analysis showed that marmoset AOX1 was closely clustered with primate AOX1s, unlike non-primate animal model AOX1s of pig, rabbit, rat, and mouse, used in drug metabolism. The tissue expression analyses by real-time RT-PCR and immunoblotting showed that marmoset AOX1 mRNA and protein were abundantly expressed in livers, similar to cynomolgus monkeys and humans. Marmoset AOX1 heterologously expressed in *Escherichia coli* catalyzed the oxidation of carbazeran and phthalazine, typical AOX1 substrates, similar to cynomolgus monkey and human AOX1s. Human and marmoset AOX1 effectively catalyzed phthalazine oxidation when assessed with Michaelis-Menten kinetics, but cynomolgus monkey AOX1 catalyzed this reaction with cooperative kinetics with high capacity. These results indicated that tissue distribution and enzymatic function of AOX1 enzyme is similar between marmosets and humans, suggesting that marmosets are a suitable primate model for AOX-dependent drug metabolism in preclinical studies.

DMD Fast Forward. Published on May 9, 2017 as DOI: 10.1124/dmd.117.076042
This article has not been copyedited and formatted. The final version may differ from this version.

Introduction

The Old World primates, cynomolgus monkeys (*Macaca fascicularis*) and rhesus monkeys (*Macaca mulatta*), and the New World primate, common marmosets (*Callithrix jacchus*), have been widely used (Uno et al., 2016) and have shown potential (Sasaki, 2015) as non-human primate models in preclinical testing of drug candidates. Aldehyde oxidase (AOX, EC 1.2.3.1) is a molybdenum cofactor-containing drug-metabolizing enzyme involved in the oxidation of a variety of aldehydes and heterocyclic-containing drug molecules (Garattini et al., 2009). Marked interspecies differences of AOX activities in livers have been reported (Garattini and Terao, 2012) resulting in a lack of clinical translation of candidate drugs attributed to decreased rat AOX activity or missing dog *AOX* gene (Crouch et al., 2017). Oxidation activities of *N*-phenylquinolinium chloride in rat and dog livers have been shown to be low and negligible, respectively, whereas baboon livers have showed high aldehyde oxidase activity; these oxidation activities by marmoset and guinea pig livers are reportedly similar to human livers (Beedham et al., 1987). A selective inhibitor of the sodium/hydrogen exchanger, zoniporide, have been converted to 2-oxozoniporide in liver cytosolic fractions from humans and rats, but not dogs (Dalvie et al., 2010). In terms of cytochrome P450 (EC 1.14.14.1) catalytic function, marmosets could be one of the animal models for human drug metabolism (Uno et al., 2016). On the other hand, the establishment of appropriate surrogate animal species for AOX-dependent drug metabolism has been desired, but little information is available about the molecular characteristics of marmoset AOX.

In this study, we isolated marmoset AOX1 cDNA based on the marmoset genome and analyzed the tissue expression specificity and catalytic activity using recombinant AOX protein. This work

provides information about the molecular basis and characteristics of marmoset AOX1 for the utilization of marmosets in pharmacokinetic and toxicokinetic preclinical testing.

DMD Fast Forward. Published on May 9, 2017 as DOI: 10.1124/dmd.117.076042
This article has not been copyedited and formatted. The final version may differ from this version.

Materials and Methods

Chemicals and enzymes

Phthalazine and phthalazone were purchased from Tokyo Kasei (Tokyo, Japan). Carbazeran and 4-hydroxycarbazeran were purchased from Toronto Research Chemicals (Toronto, Canada). All DNA oligonucleotides were supplied by Sigma Genosys (Ishikari, Japan). Caucasian liver cytosolic fractions pooled from 10 humans (mixed gender) previously prepared (Shimada et al., 1994) were used under the approval of the ethics committee of Showa Pharmaceutical University. Marmoset liver cytosolic fractions were prepared from 10 marmosets (9 males and 1 female, >2 years of age) raised at the Central Institution for Experimental Animals (Kawasaki, Japan). Liver cytosolic fractions were also prepared from cynomolgus monkeys (10 males, 3-8 years old, Shin Nippon Biomedical Laboratories, Ltd., Kainan, Japan) and dogs (2 males, sexually mature; Xenotech Lenexa, KS). Brain, lung, liver, kidney, and jejunum tissues were obtained from marmosets, and brain, lung, heart, liver, kidney, jejunum, adrenal gland, testis, ovary, uterus, and nasal tissues were also collected from cynomolgus monkeys. This study was reviewed and approved by the Institutional Animal Care and Use Committees of the Central Institution for Experimental Animals and Shin Nippon Biomedical Laboratories, Ltd. Anti-human AOX1 antibodies (ab197828) and goat anti-rabbit IgG-horseradish peroxidase (A0545) were purchased from Abcam (Cambridge, MA) and Sigma-Aldrich, respectively. All other reagents were of the highest quality commercially available.

AOX1 cDNA cloning

Human, cynomolgus monkey, and marmoset AOX1 cDNAs were cloned by (RT)-polymerase chain

reaction (PCR). Human, cynomolgus monkey, and marmoset liver cDNAs were prepared with total RNA extracted from livers using SuperScript III RT reverse transcriptase (Invitrogen, Carlsbad, CA), oligo (dT) primer (Invitrogen), and RNase OUT (Invitrogen) following the manufacturer's instructions. PCR was performed using KOD-Plus-Neo DNA polymerase (Toyobo, Osaka, Japan) with an ABI GeneAmp PCR System 9700 thermocycler (Applied Biosystems, Foster City, CA). PCR conditions consisted of an initial denaturation step at 98°C for 2 minutes, 35 cycles of denaturation at 98°C for 15 seconds, annealing at 65°C for 30 seconds, and extension at 68°C for 2.5 minutes, and a final extension at 68°C for 7 minutes. PCR primers were designed based on genome sequences of humans, cynomolgus monkeys, and marmosets; hAOX1 (5rt1) 5′-ATGGACCGGGCGTCCGAGCTGCTCTTC-3′ and hAOX1 (3rt1) 5′-GATTGCCATCTGGGAAGAGGCACTCTGTTTTCTC-3′ for human AOX1, mfAOX1 (5rt1) 5′-CAATGGACAGGGCGTCCGAACTGCT-3′ and mfAOX1 (3rt1) 5′-CATTGCCATCTGGGAAGAGGCACTCCA-3′ for cynomolgus monkey AOX1, and cjAOX1 (5rt1) 5′-ATGGACCGGACGCCGGAGCTGCTCTTCTAC-3′ and cjAOX1 (3rt1) 5′-CTGCCGTCTGGGAAGGCATGCCATTTTCTC-3′ for marmoset AOX1. PCR products were purified and cloned into pCR4 vectors using a Zero Blunt TOPO PCR Cloning Kit for Sequencing (Invitrogen). Insert DNA fragments were sequenced with an ABI PRISM 3730 DNA Analyzer (Applied Biosystems).

Enzyme assay

Phthalazine oxidation activities by recombinant AOX proteins and liver cytosolic fractions were measured by HPLC (Prominence-I LC-2030C HPLC system, Shimadzu, Kyoto, Japan) as described

previously (Panoutsopoulos and Beedham, 2004) with some minor changes. Briefly, the incubation mixture consisted of AOX1 protein (arbitrary volume) or 0.50 mg/mL liver cytosolic fractions, 0.44-80 μM phthalazine, and 100 μM potassium phosphate buffer (pH 7.4) in a total volume of 0.25 mL. The reaction was incubated at 37°C for 3 min and terminated with 25 μL of 60% trichloroacetic acid. The resultant solutions were centrifuged at 10,000g for 5 min. Supernatants (100 μL) were analyzed by reversed-phase HPLC on a C_{18} column (5 μm, 250 × 4.6 mm, Mightysil aqua) using a mobile phase gradient consisting of acetonitrile and 0.1% acetic acid at a flow rate of 1.2 mL/min with ultraviolet monitoring at 285 nm. The gradient elution conditions were 0% acetonitrile (0–7 minutes), 10–15% acetonitrile (15–19 minutes), 15% acetonitrile (19–23 minutes), and 0% acetonitrile (23.1–30 minutes). The standard calibration curve indicated linearity over the concentration range of 0.20–150 μg/ml of phthalazone. The enzymatic activities were calculated based on the standard curve prepared with dilution series of parent drug phthalazone. Kinetic parameters for phthalazine oxidation were estimated from the fitted curves employing Michaelis-Menten equations or Hill equations using the KaleidaGraph program (Synergy Software, Reading, PA). Carbazeran oxidation activities by recombinant AOX proteins and liver cytosolic fractions were measured by an HPLC system coupled with an API4000 (AB Sciex, Foster City, CA) as described previously (Kaye et al., 1985; Manevski et al., 2014) with some minor changes. Briefly, the incubation mixtures consisted of approximately 40 pmol/mL AOX1 protein (arbitrary volume) or 0.50 mg/mL liver cytosolic fractions, 5.0 μM carbazeran, and 100 μM potassium phosphate buffer (pH 7.4) in a total volume of 0.25 mL. The reaction was incubated at 37°C for 2.5 min and terminated with 500 μL of acetonitrile containing 5 μM dextrorphan as an internal standard. The resultant solutions were centrifuged at 10,000 *g* for 5 min. Supernatants (5-10 μL) were analyzed by reversed-phase HPLC on a C_{18} column

(3 μm, 2.0 × 3.5 mm, Cadenza CD-C18) using an isocratic mobile phase [0.1% formic acid in water and 0.1% formic acid in acetonitrile (80:20, v/v)] at a flow rate of 0.2 mL/min. The metabolite and internal standard were detected in the positive ion electrospray ionization mode and identified using the transitions *m/z* 377.2→288.1 for 4-hydroxycarbazeran and *m/z* 258.1→157.1 for dextrorphan. The peak area ratio of the analyte versus the internal standard was determined for each injection sample and used to quantify the amount of metabolite formed. The standard calibration curve indicated linearity over the concentration range of 4.0–1000 ng/ml. The enzymatic activities were calculated based on standard curves prepared with dilution series of 4-hydroxycarbazeran.

Results and Discussion

The homology search of the genome sequences of the common marmoset showed *AOX1*, *AOX2*, and *AOX4* genes were localized in the *AOX* gene cluster in marmoset chromosome 6 (Supplemental Fig. 1). Multiple *AOX* genes contained complete open reading frames in rats, dogs, marmosets, and cynomolgus monkeys, unlike humans. Among experimental animals, *AOX1* gene was a pseudogene in dogs, different from cynomolgus monkeys, marmosets, and rats. The presence of *AOX3* gene in marmosets was not determined clearly because of the five large gaps (>1900 bp) between *AOX1* and *AOX4* genes (Supplemental Fig. 1). Marmoset AOX1 cDNA from livers were successfully cloned by RT-PCR. Marmoset AOX1 cDNA contained the open reading frame of 1337 amino acid residues, including highly conserved amino acids involved in the interactions with the 2Fe-2S prosthetic groups, the FAD cofactor (the molybdenum cofactor), and characteristic and functional key residues of AOX proteins (Supplemental Fig. 2). The exon-intron structure of marmoset *AOX1* gene was determined using BLAT by aligning the marmoset AOX1 cDNA sequence with the marmoset genome. Marmoset *AOX1* gene spanned >89.7 kb and consisted of thirty-five exons (Supplemental Table 1), similar to cynomolgus monkey and human *AOX1* genes. The sizes of exons and introns ranged from ≥45 to 228 bp and 301 to ≥10775 bp, respectively. The results indicated that marmoset *AOX1* possesses a similar gene structure to *AOX1* of cynomolgus monkeys and humans. Deduced amino acids of marmoset AOX1 cDNA showed high sequence identities with primate AOX1 (92–93%) (Table 2), but to a lesser extent with pig (85%), rabbit (82%), rat (81%), and mouse (82%) AOX1. Phylogenetic analysis indicated that marmoset AOX1 was more closely clustered with human AOX1 than pig, rabbit, and rodent AOX1 (Supplemental Fig. 3). These results

suggest an evolutionary closeness of marmoset AOX1 to human AOX1 as compared with AOX1 of non-primate species.

Tissue distribution of AOX1 mRNAs in marmosets and cynomolgus monkeys was investigated by real-time RT-PCR. Marmoset AOX1 mRNA was the most abundant in livers among brains, lungs, livers, kidneys, and small intestines (Supplemental Fig. 4A). Cynomolgus monkey AOX1 mRNA was also most abundant in livers, followed by adrenal glands (Supplemental Fig. 4B), among eleven tissues. Similarly, AOX1 mRNA was abundant in livers and adrenal glands among 23 human tissues (Nishimura and Naito, 2006). Additionally, the protein expression of liver cytosolic AOX1 was investigated by immunoblotting using anti-human AOX1 antibodies cross-reacting with AOX1 of marmosets and cynomolgus monkeys (Fig. 1). AOX1 proteins (~150 kDa) were immunologically detected in liver cytosolic fractions from humans, rhesus monkeys, cynomolgus monkeys, and marmosets, but not dogs (Fig. 1A). AOX1 proteins were expressed in individual liver cytosolic fractions from marmosets, cynomolgus monkeys, and rhesus monkeys (Fig. 1B, 1C). In cynomolgus monkeys, AOX1 protein expression levels in liver cytosolic fractions were not substantially different between the animals bred in Cambodia, China, and Indonesia (Fig. 1B). These results suggested that the tissue distribution of AOX1 is similar between marmosets, cynomolgus monkeys, and humans.

To assess catalytic activities of marmoset AOX1, phthalazine and carbazeran oxidation activities by marmoset liver cytosolic fractions and recombinant AOX1 protein were measured. Phthalazine and carbazeran oxidation activities by liver cytosolic fractions from marmosets and cynomolgus monkeys were higher than those of humans (Supplemental Table 3). Kinetic analyses for phthalazine oxidations were performed using liver cytosolic fractions from humans, cynomolgus monkeys, and

DMD Fast Forward. Published on May 9, 2017 as DOI: 10.1124/dmd.117.076042
This article has not been copyedited and formatted. The final version may differ from this version.

marmosets and recombinant AOX1 enzymes (Table 1, Supplemental Fig. 5). Liver cytosolic fractions from humans and marmosets showed Michaelis-Menten kinetics with comparable low K_m values (4.7 μM for humans, 5.7 μM for marmosets) and different V_{max} values (0.11 nmol/min/mg protein for humans, 5.0 nmol/min/mg protein for marmosets) (Table 1, Supplemental Fig. 5A and 5E). Marmoset AOX1 enzyme had high affinity (K_m values, 1.3 μM) for phthalazine oxidation, comparable to liver cytosolic fractions from marmosets, suggesting AOX1 is a major aldehyde oxidase in marmoset livers (Table 1, Supplemental Fig. 5B and 5F). Because precise molecular expression levels in histidine-tagged AOX protein were unknown under any standard proteins, the arbitrary units were applied in this study (Table 1). On the other hand, liver cytosolic fractions from cynomolgus monkeys showed cooperative kinetics for phthalazine oxidation with high V_{max} values (83 nmol/min/mg protein) (Table 1, Supplemental Fig. 5C). Cooperativity was also observed in recombinant cynomolgus monkey AOX1 (Table 1, Supplemental Fig. 5D).

A recent report has indicated that cynomolgus monkeys are a suitable surrogate model for AOX metabolism of the EGFR inhibitor BIBX1382 in terms of its *in vivo* clearance and metabolite profile (Hutzler et al., 2014). AOX-dependent oxidation of a multityrosine kinase inhibitor lenvatinib has been catalyzed by liver 9000 *g* supernatant fractions from only cynomolgus monkeys and humans, but not by those of rats or dogs (Inoue et al., 2014). The predicting of human *in vivo* clearance values by scaling using *in vitro* intrinsic clearance values of five AOX substrates indicated that guinea pigs and monkeys reportedly represent better models of AOX-mediated drug clearances in humans (Crouch et al., 2017). Therefore, these differences of kinetics for AOX1-dependent phthalazine oxidation in liver cytosolic fractions between humans and cynomolgus monkeys might be minor

species differences. *In vitro* hepatic oxidation activities of *N*-phenylquinolinium chloride catalyzed by AOX were similar to human in marmosets and guinea pigs, unlike rats, guinea pig, dogs, and baboons (Beedham et al., 1987). In this study, marmoset liver cytosol and recombinant marmoset AOX1 metabolized human AOX1 substrates, phthalazine and carbazeran (Table 1, Supplemental Table 3). These results indicated the similarity of enzymatic functions between human and marmoset AOX1 enzymes, suggesting that marmosets would also be a suitable primate model for AOX-dependent drug oxidation in preclinical testing.

In conclusion, we identified a novel AOX1 in marmosets, highly homologous to AOX1 of other primate species. Although *in vivo* pharmacokinetics of representative human AOX substrates in the marmoset have not been currently investigated, similar tissue expression patterns and oxidation activities towards carbazeran and phthalazine (a typical human AOX1 substrate) of marmoset AOX1 to human AOX1 suggest functional similarities of AOX-dependent drug oxidations between marmosets and humans *in vitro* situation.

Authorship contribution

Participated in research design: Uehara, Uno, and Yamazaki.

Conducted experiments: Uehara, Uno, and Okamoto.

Contributed new reagents or analytic tools: Inoue and Sasaki.

Performed data analysis: Uehara, Uno, and Yamazaki.

Wrote or contributed to the writing of the manuscript: Uehara, Uno, and Yamazaki.

References

Beedham C, Bruce SE, Critchley DJ, al-Tayib Y, and Rance DJ (1987) Species variation in hepatic aldehyde oxidase activity. *Eur J Drug Metab Pharmacokinet* **12:**307-310.

Crouch RD, Hutzler JM, and Daniels JS (2017) A novel in vitro allometric scaling methodology for aldehyde oxidase substrates to enable selection of appropriate species for traditional allometry. *Xenobiotica*, in press.

Dalvie D, Zhang C, Chen W, Smolarek T, Obach RS, and Loi CM (2010) Cross-species comparison of the metabolism and excretion of zoniporide: contribution of aldehyde oxidase to interspecies differences. *Drug Metab Dispos* **38:**641-654.

Garattini E, Fratelli M, and Terao M (2009) The mammalian aldehyde oxidase gene family. *Hum Genomics* **4:**119-130.

Garattini E and Terao M (2012) The role of aldehyde oxidase in drug metabolism. *Expert Opin Drug Metab Toxicol* **8:**487-503.

Hartmann T, Terao M, Garattini E, Teutloff C, Alfaro JF, Jones JP, and Leimkuhler S (2012) The impact of single nucleotide polymorphisms on human aldehyde oxidase. *Drug Metab Dispos* **40:**856-864.

Hutzler JM, Cerny MA, Yang YS, Asher C, Wong D, Frederick K, and Gilpin K (2014) Cynomolgus monkey as a surrogate for human aldehyde oxidase metabolism of the EGFR inhibitor BIBX1382. *Drug Metab Dispos* **42:**1751-1760.

Inoue K, Mizuo H, Kawaguchi S, Fukuda K, Kusano K and Yoshimura T (2014) Oxidative metabolic pathway of lenvatinib mediated by aldehyde oxidase. *Drug Metab Dispos* **42**:1326-1333.

Kaye B, Rance DJ, and Waring L (1985) Oxidative metabolism of carbazeran in vitro by liver cytosol of baboon and man. *Xenobiotica* **15:**237-242.

Manevski N, Balavenkatraman KK, Bertschi B, Swart P, Walles M, Camenisch G, Schiller H, Kretz O, Ling B, Wettstein R, Schaefer DJ, Pognan F, Wolf A, and Litherland K (2014) Aldehyde oxidase activity in fresh human skin. *Drug Metab Dispos* **42:**2049-2057.

Nishimura M and Naito S (2006) Tissue-specific mRNA expression profiles of human phase I metabolizing enzymes except for cytochrome P450 and phase II metabolizing enzymes. *Drug Metab Pharmacokinet* **21:**357-374.

Panoutsopoulos GI and Beedham C (2004) Enzymatic oxidation of phthalazine with guinea pig liver aldehyde oxidase and liver slices: inhibition by isovanillin. *Acta Biochim Pol* **51:**943-951.

Sasaki E (2015) Prospects for genetically modified non-human primate models, including the common marmoset. *Neurosci Res* **93:**110-115.

Shimada T, Yamazaki H, Mimura M, Inui Y, and Guengerich FP (1994) Interindividual variations in human liver cytochrome P-450 enzymes involved in the oxidation of drugs, carcinogens and toxic chemicals: studies with liver microsomes of 30 Japanese and 30 Caucasians. *J Pharmacol Exp Ther* **270:**414-423.

Uno Y, Uehara S, and Yamazaki H (2016) Utility of non-human primates in drug development: Comparison of non-human primate and human drug-metabolizing cytochrome P450 enzymes. *Biochem Pharmacol* **121:**1-7.

Footnotes

Shotaro Uehara and Yasuhiro Uno equally contributed.

This work resulted from "Construction of System for Spread of Primate Model Animals" under the Strategic Research Program for Brain Sciences of Japan Agency for Medical Research and Development. Shotaro Uehara was also supported partly by the Japan Society for the Promotion of Science Grant-in-Aid for Young Scientists B [15K18934].

DMD Fast Forward. Published on May 9, 2017 as DOI: 10.1124/dmd.117.076042
This article has not been copyedited and formatted. The final version may differ from this version.

Legends for figures

Fig. 1. Immunochemical detection of AOX1 proteins in liver cytosolic fractions from marmosets and cynomolgus monkeys.

Anti-human AOX1 antibodies cross-reacted with AOX1 proteins in liver cytosolic fractions (20 μg) from marmosets, cynomolgus monkeys, and humans, but not in liver cytosolic fractions from dogs (A). AOX1 proteins were detected in individual liver cytosolic fractions from 9 cynomolgus monkeys (lanes 1-3, bred in China; lanes 4-6, bred in Indonesia; lanes 7-9, bred in Indonesia), 3 rhesus monkeys (lanes 9-11) (B) and 10 marmosets (C). Anti-human AOX1 antibodies cross-reacted with recombinant histidine-tagged AOX1 proteins (20 μg) of marmosets, cynomolgus monkeys, and humans (D).

Table 1. Kinetic parameters for phthalazine oxidations by liver cytosolic fractions from marmosets, cynomolgus monkeys, and recombinant AOX1 enzymes

Enzyme source	K_m or S_{50}	Hill coefficient	V_{max}	V_{max}/K_m or V_{max}/S_{50}
Liver cytosolic fraction	*μM*		*nmol/min/mg protein*	*mL/min/mg protein*
Humans	4.7 ± 1.6	-	0.11 ± 0.01	0.023
Cynomolgus monkeys	32 ± 6	1.4 ± 0.2	83 ± 9	2.6
Marmosets	5.7 ± 0.3	-	5.0 ± 0.1	0.88
Recombinant enzymes	*μM*		*nmol/min/arbitrary units* [a]	*mL/min/arbitrary units* [a]
Human AOX1	23 ± 2	-	6.5 ± 0.2 (2.3[b])	0.28
Cynomolgus monkey AOX1	5.8 ± 0.3	1.3 ± 0.1	69 ± 1	12
Marmoset AOX1	1.3 ± 0.3	-	1.4 ± 0.1	1.1

Kinetic parameters were determined by non-linear regression analysis (mean ± standard error, n = 14 points of substrate concentrations of 0.44–80 μM, in duplicate determinations) employing the equation, $v = V_{max} \times [S]/(K_m + [S])$ for Michaelis-Menten equation and $v = V_{max} \times [S]^n/([S_{50}]^n + [S]^n)$ for Hill equation. [a] Relative phthalazine oxidation activities were shown on the bases of recombinant human AOX1 activity (at substrate concentration of 5.0 μM) as 1, because of unknown precise molecular expression level without standard proteins. [b] A number in parenthesis (2.3 nmol/min/nmol of AOX1) was a reported V_{max} value (Hartmann et al., 2012) for phthalazine oxidation by recombinant human AOX1.

DMD Fast Forward. Published on May 9, 2017 as DOI: 10.1124/dmd.117.076042
This article has not been copyedited and formatted. The final version may differ from this version.

Figure 1

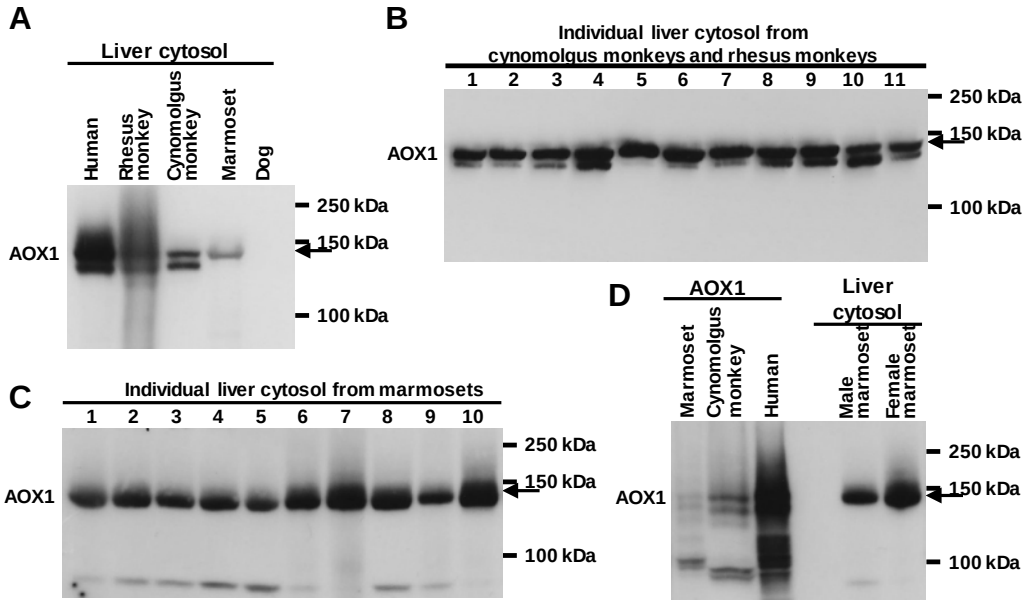

Supplemental Data

Molecular cloning and characterization of marmoset aldehyde oxidase

Shotaro Uehara, Yasuhiro Uno, Eriko Okamoto, Takashi Inoue, Erika Sasaki, and Hiroshi Yamazaki

Drug Metabolism and Disposition

Supplemental Methods

Bioinformatics

The structure of *AOX* gene cluster was determined using genome sequences from various species in BLAT (UCSC Genome Bioinformatics, Santa Cruz, CA). The homology comparison of nucleotide and amino acid sequences was analyzed using BLAST (National Center for Biotechnology Information, Bethesda, MD). Multiple sequences were aligned using Genetyx (Software Development, Tokyo, Japan). Phylogenetic trees were constructed using the DNASIS Pro (Hitachi Software, Tokyo, Japan). The amino acid sequences of AOXs from various species were obtained from GenBank: human AOX1 (NP_001150); chimpanzee AOX1 (NP_001295372); gorilla AOX1 (NP_001266605); orangutan AOX1 (NP_001125740); baboon AOX1 (NP_001289031), AOX2 (NP_001295367), and AOX4 (NP_001295365); cynomolgus monkey AOX1 (NP_001271673), AOX2 (NP_001295329), and AOX4 (NP_001295332); rhesus monkey AOX1 (NP_001268238), AOX2 (NP_001268244), and AOX4 (NP_001305103); marmoset AOX1 (NP_001295373); dog AOX2 (NP_001041597) and AOX4 (NP_001038214); pig AOX1 (NP_001295402) and AOX2 (NP_001295401); rabbit AOX1 (NP_001075459), AOX2 (NP_001284417), AOX3

(NP_001295389), and AOX4 (NP_001265792); guinea pig AOX1 (NP_001295371), AOX2 (NP_001265693), and AOX4 (NP_001265709); rat AOX1 (NP_062236), AOX2 (NP_001008522), AOX3 (NP_001008527), and AOX4 (NP_001008523); mouse AOX1 (NP_033806), AOX2 (NP_001008419), AOX3 (NP_076106), and AOX4 (NP_076120); and *nocardia elegans* AOX (WP_063028309).

Real-time RT-PCR

The expression level of AOX1 mRNA in five tissues (brain, lung, liver, kidney, and jejunum) of marmosets and eleven tissues (brain, lung, heart, liver, kidney, jejunum, adrenal gland, testis, ovary, uterus, and nasal mucosa) of cynomolgus monkeys were determined by real-time RT-PCR. Total RNA of each pooled tissues from marmosets and cynomolgus monkeys was reverse-transcribed into the first-strand cDNA with SuperScript III RT reverse transcriptase, random primers (Invitrogen), and RNase OUT following the manufacturer's instructions. Real-time PCR was carried out using Power SYBR Green Master Mix (Applied Biosystems) with the ABI PRISM 7300 sequence detection system (Applied Biosystems). The final concentration of each primer was 200 nM. PCR conditions consisted of an initial denaturation step at 50°C for 2 minutes, 95°C for 10 minutes, 40 cycles 95°C for 15 seconds and 60°C for 1 minute. The dissociation curve was obtained after the cycle of the PCR reaction at 95°C for 15 seconds. PCR primers used were XXXX 5′-GTTTGGAGGGAAGGTGTTCA-3′ and XXXX 5′-GGAGGTGCCTGCATTGTTAT-3′ for marmoset AOX1 and mfAOX1 (5qrt1) 5′-GATCTGTCAGAAGCTCTCAGCAT-3′ and mfAOX1 (3qrt1) 5′- TGACCCACACAGAACACCTTATC-3′ for cynomolgus monkey AOX1. As reference gene we used 18S rRNA in order to normalize the expression of the analyzed genes. All reactions were performed in triplicate.

Heterologous protein expression in *Escherichia coli*

Human, cynomolgus monkey, and marmoset AOX1 cDNA containing the entire open reading frame was inserted into pQE-30 Xa expression vectors (Qiagen, Valencia, CA), overexpressed as an *N*-terminal 6x-His-tag in an *Escherichia coli* (*E. coli*) strain, XL-1 Blue as described previously with minor changes (Alfaro et al., 2009). Briefly, a single colony was picked and grown overnight in LB broth (100 μg/ml ampicillin, 1 μg/ml riboflavin, and 50 μM sodium molybdate). The overnight culture was used to inoculate 200 mL of Terrific broth (100 μg/mL ampicillin, 250 μL of trace element solution containing 2.7 g of $FeCl_3 \cdot 6H_2O$, 0.13 g of $ZnCl_2$, 0.20 g of $CoCl_2 \cdot 6H_2O$, 0.15 g of $Na_2MoO_4 \cdot 2H_2O$, 0.10 g of $CaCl \cdot 2H_2O$, 0.12 g of $CuCl_2 \cdot 2H_2O$, 0.05 g of H_3BO_3, and 10 mL of concentrated HCl autoclaved in a total volume of 100 mL ultrapure water, 1 μg/mL riboflavin, and additional 50 μM sodium molybdate). Cultures were incubated at 37°C and 200 rpm until an absorbance of 0.6 at 600 nm, and then isopropyl-D-thiogalactoside (1 mM) were added for induction. Cells continued to grow at 25°C for 72 hours at 150 rpm. After collection by centrifugation at 7000×g for 10 minutes at 4 °C, the cells were sonicated on ice. Histidine-tagged recombinant AOX proteins were purified using ProBond Purification System (Invitrogen) according to the manufacturer's instructions. The contents of marmoset, cynomolgus monkey, and human AOX proteins were semi-quantified by immunoblotting using anti-human AOX1 antibodies.

Immunoblotting

The expression of AOX1 proteins were analyzed with liver cytosolic fractions from humans, cynomolgus monkeys, rhesus monkeys, marmosets, and dogs by immunoblotting with anti-human AOX1 antibodies (ab197828, Abcam, Cambridge, MA). Recombinant histidine-tagged AOX proteins and liver cytosols (20 μg) were separated by 10% sodium dodecyl sulfate-polyacrylamide gel electrophoresis and then transferred on polyvinylidene difluoride membranes (Merck Millipore, Billerica, MA). Non-specific binding was blocked

with 0.5% nonfat milk in TBS (50 mM Tris, 138 mM NaCl, and 2.7 mM KCl) containing 0.05% Tween 20 (v/v) (TBST). Membranes were probed at room temperature for 1 hour with the primary antibodies diluted in blocking buffer at 1:1000 dilution. After 30 minutes of washes with TBST, membranes were probed for 20 minutes at room temperature with the secondary antibodies diluted in blocking buffer at 1:5000 dilution. After 30 minutes of washes with TBST, bands were visualized by enhanced chemiluminescence with an ECL Prime Western Blotting Detection System (GE Healthcare, Buckinghamshire, UK).

References

Alfaro JF, Joswig-Jones CA, Ouyang W, Nichols J, Crouch GJ, and Jones JP (2009) Purification and mechanism of human aldehyde oxidase expressed in Escherichia coli. *Drug Metab Dispos* **37:**2393-2398.

Supplemental Table 1

Exon-intron boundary sequences of the marmoset *AOX1* gene.

Exon	Exon size (bp)	3′ splice site	5′ splice site	Intron size (bp)
1	≥45		CCGCAAGgtgagcgcc	7004
2	58	ttggtatagGTGACAG	GAATAAGgtaccgtgt	2055
3	97	ctcttccagTCCGACT	GAATAAGgtaccgtgt	3712
4	109	attctgaagGCATCAC	TGTTCAGgtgaggatg	≥2258
5	127	tgcttccagGAGAGGA	CTTGGTGgtaggtt	2796
6	62	ctccttcagGTAACCT	CTGTAAAgtaagtgga	946
7	90	gtccactagACTTCAG	AAGTGAGgtcagtgaa	655
8	81	ctttttaagACGAGTC	GCTAATGgtaagtaaa	607
9	145	tttcaatagGTAATGG	TCTGTGGgtatgtaga	685
10	93	atcctttagGGCCTGA	TCTACTGgtgagttcc	3361
11	152	tcatttcagGACTCAC	CATGGCTgtatgtatc	189
12	94	tttaaaaagTCTTTAG	TCAAAAGgtaagtgac	2208
13	110	tttccacagAAGGAAA	AAGGAAGgtgagaaca	734
14	185	ttctttcagTGGGAAT	TTGGAAGgtaaggcat	931
15	163	actttctagGCTCTGG	AAAGATGgtacacatt	1969
16	93	acttttcagAACTCAG	GTACCAGgtgagtg	4576
17	170	attaaatagAAAATAG	AGATTGTgtaagtgat	301
18	127	accacctagGTCTATT	AGATAAGgtactgcat	2563
19	123	gtgtcgtagGTGTTCT	AATTGAGgtaatgaat	2821
20	97	tctttctagGAAGCTA	CTTGAAGgtaaagaag	6717
21	125	ctgtaacagGTGAAAT	TATACAGgtaacatgg	1957
22	134	tgttcacagGACATAG	CAAACAAgtaagtgga	1279
23	88	ctgttttagACATGGC	GTACAAAgtaagtata	3042
24	113	cttccccagGCTGGAT	AGTTAACgttcctgaa	≥1901
25	163	ctctgaaatGGACATG	CGAGAAGgtaatacta	≥10775
26	228	ctttcatagGTGCGAA	TGGTCAGgtcagttct	5566
27	96	tctgctcagGCTGCTG	GATTCAGgtaagaatg	2271
28	129	aaaatccagGTGGCCA	AGTAAAGgtaacagtc	≥659
29	75	aatttctagGATGCCT	AGACTGGgtgagaatc	1544
30	53	ccttcatagGCGGAGA	ACTTCAGgtaaatact	1224
31	115	ttcctccagGGGTTAT	TCATAAGgtcagtact	3637
32	66	tattactagAACATCA	CGGCCAGgtacatgta	1498
33	189	ttgcctcagATTGAAG	ATCTAAGgtaagttac	774
34	168	cccttcaagGGTCTGG	AAAAATGgtatgttct	879
35	≥51	ttatcctagATTCCAA		

Exon and intron sequences are shown in capital and lower case letters, respectively.

Supplemental Table 2

Sequence identity of AOX1 cDNA and amino acids for marmosets as compared to other species.

Species	Identity (%)	
	cDNA	Amino acids
Human	94	93
Chimpanzee	94	93
Gorilla	94	92
Orangutan	94	93
Baboon	94	92
Cynomolgus monkey	94	92
Rhesus monkey	94	92
Pig	87	85
Rabbit	84	82
Rat	83	81
Mouse	83	82

Supplemental Table 3

Carbazeran oxidation activities by liver cytosolic fractions from marmosets, cynomolgus monkeys, and humans and recombinant AOX1 enzymes

Enzyme source	Carbazeran oxidation activity
Liver cytosolic fractions	*nmol/min/mg protein*
Humans	0.12 ± 0.01
Cynomolgus monkeys	14 ± 1
Marmosets	2.2 ± 0.1
Recombinant enzymes	*nmol/min/arbitrary units* [a]
Human AOX1	1.0 ± 0.1
Cynomolgus monkey AOX1	75 ± 7
Marmoset AOX1	9.8 ± 0.9

Catalytic activities were measured at a substrate concentration of 5.0 μM carbazeran. Data represent the mean ± SD in triplicate determinations (for technical reproducibility). [a] Adjusted relative oxidation activities were shown on the bases of recombinant human AOX1 as 1.

Supplemental Fig. 1. *AOX* genes in mammalians.

Direction of each gene is indicated by arrows. Solid arrows indicate the expressed genes containing a complete open reading frame. Shorter open arrows indicate pseudogenes. Shaded arrows indicate the genes that have a complete or nearly complete open reading frame, but their expressions have not been reported. Sizes of the genes and the distance between the genes are not proportionate to the actual measurement. A broken line indicates the region containing multiple large gaps.

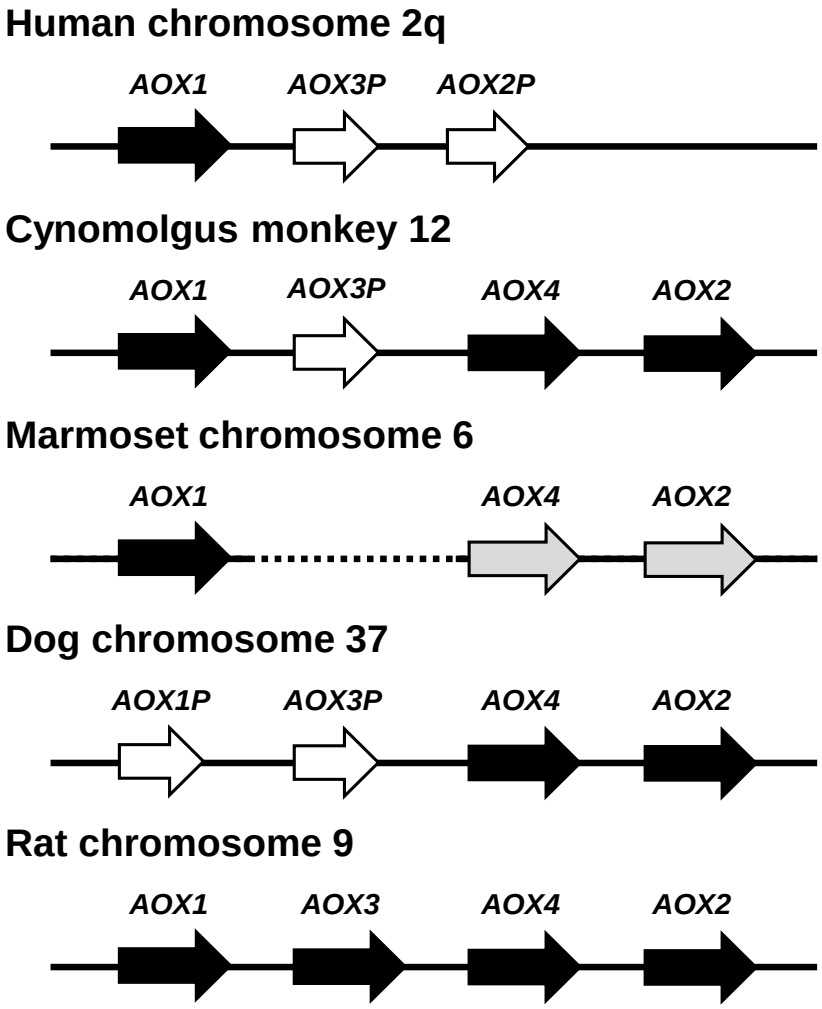

Supplemental Fig. 2. Alignment of AOX1 amino acid sequences from experimental animals.

AOX1 amino acid sequences from marmosets (cj), humans (h), cynomolgus monkeys (mf), rats (r), and mice (m) were aligned using Genetyx. Regions conserved and roughly conserved among the five species are shown asterisks and dots under amino acid alignment, respectively. Amino acids involved in the interactions with the 2Fe-2S prosthetic groups, the FAD cofactor, and the molybdenum cofactor are marked by circles, squares, and triangles, respectively.

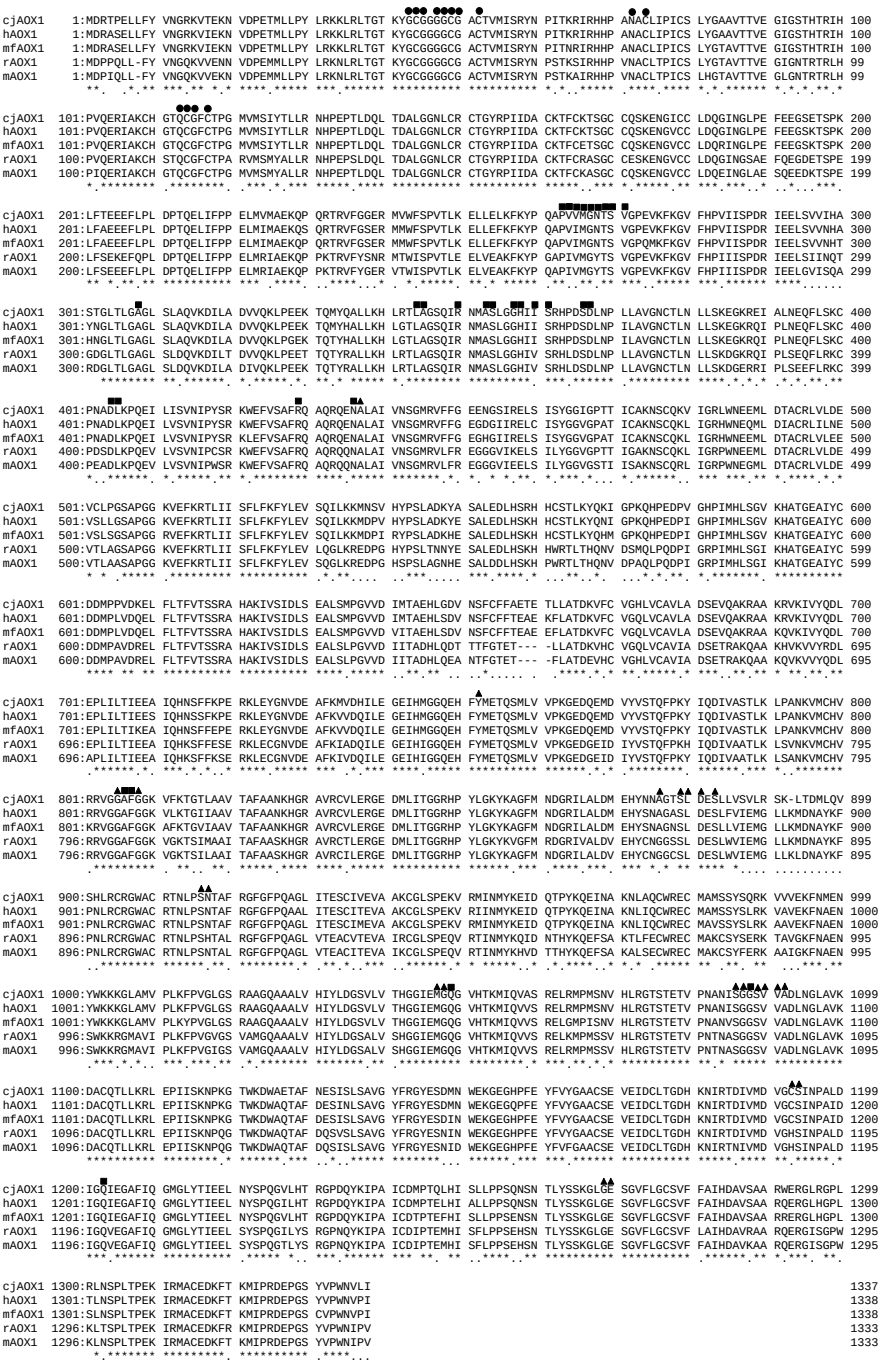

Supplemental Fig. 3. Phylogenetic analysis of AOX amino acid sequences in various species.

A phylogenetic tree was created using the neighbor-joining method based on AOX amino acid sequences of marmoset (cj), human (h), chimpanzee (ch), gorilla (g), orangutan (or), baboon (b), cynomolgus monkey (mf), rhesus monkey (mm), pig (p), dog (d), rabbit (ra), guinea pig (cp), rat (r), and mouse (m). *Nocardia elegans* AOX was used as the out group. The scale bar corresponds to 0.1 amino acid substitutions per site.

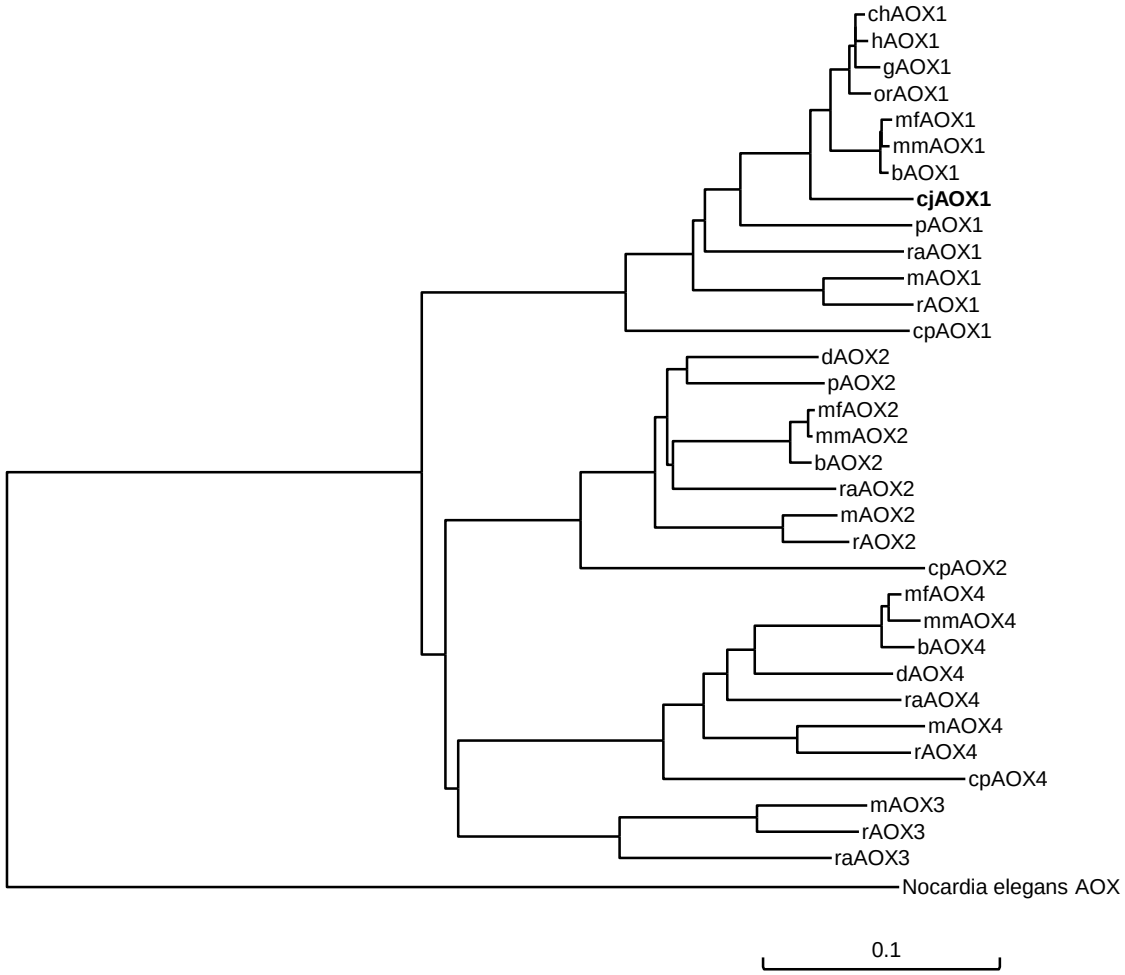

Supplemental Fig. 4. Tissue distribution of AOX1 mRNA in marmosets (A) and cynomolgus monkeys (B).

Expression levels of marmoset AOX1 mRNA in each pooled tissue from marmosets and cynomolgus monkeys were measured by quantitative real-time PCR and normalized to 18S rRNA levels. AOX1 levels in marmoset and cynomolgus monkey livers were adjusted to 1; the relative AOX1 mRNA expression levels were shown in other tissues. Data were mean in triplicate determinations (for technical reproducibility).

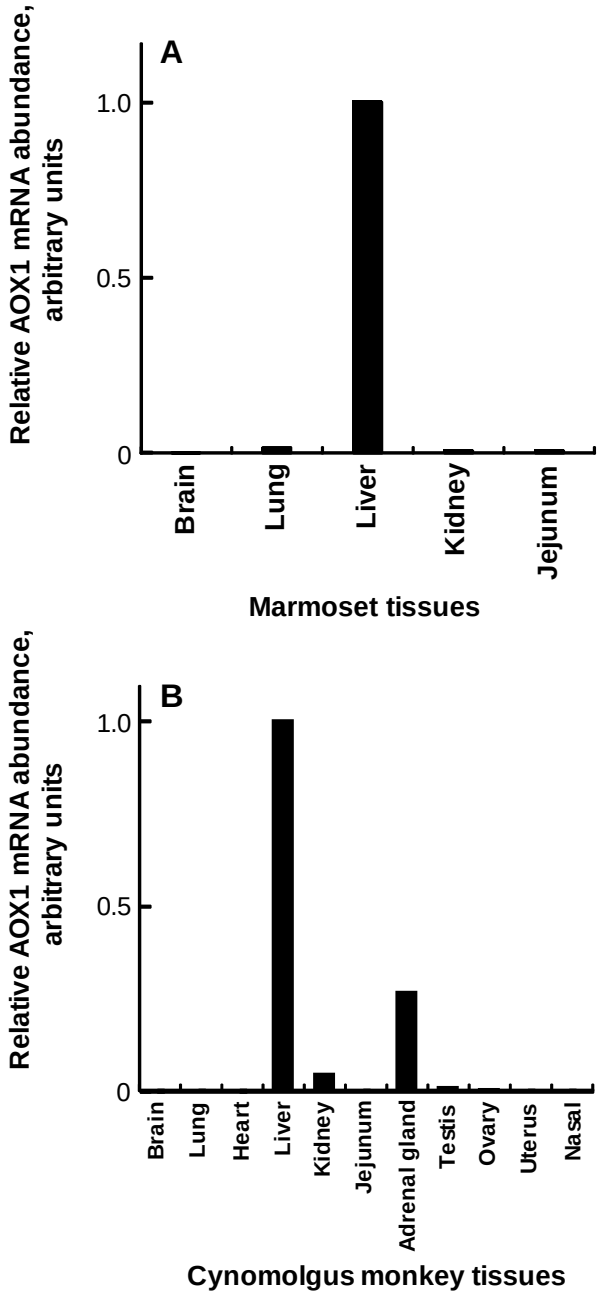

Supplemental Fig. 5. Kinetics for phthalazine oxidation by recombinant AOX1 enzymes and liver cytosols from marmosets, cynomolgus monkeys, and humans.

Kinetic analyses for phthalazine oxidation by recombinant AOX1 enzymes and liver cytosols of marmosets, cynomolgus monkeys, and humans were performed. A, human liver cytosol; B, cynomolgus monkey liver cytosol; C, marmoset liver cytosol; D, human AOX1; E, cynomolgus monkey AOX1; F, marmoset AOX1. Details are shown in the legend for Table 1.